

# IOWA STATE UNIVERSITY

## Digital Repository

---

Retrospective Theses and Dissertations

Iowa State University Capstones, Theses and  
Dissertations

---

1-1-1961

## Effect of water-cement ratio and air content on the gamma-ray absorption coefficient of concrete

Donald Phillip White  
*Iowa State University*

Follow this and additional works at: <https://lib.dr.iastate.edu/rtd>

---

### Recommended Citation

White, Donald Phillip, "Effect of water-cement ratio and air content on the gamma-ray absorption coefficient of concrete" (1961).  
*Retrospective Theses and Dissertations*. 18828.  
<https://lib.dr.iastate.edu/rtd/18828>

This Thesis is brought to you for free and open access by the Iowa State University Capstones, Theses and Dissertations at Iowa State University Digital Repository. It has been accepted for inclusion in Retrospective Theses and Dissertations by an authorized administrator of Iowa State University Digital Repository. For more information, please contact [digirep@iastate.edu](mailto:digirep@iastate.edu).

EFFECT OF WATER-CEMENT RATIO AND  
AIR CONTENT ON THE GAMMA-RAY  
ABSORPTION COEFFICIENT OF CONCRETE

by

Donald Phillip White

A Thesis Submitted to the  
Graduate Faculty in Partial Fulfillment of  
The Requirements for the Degree of  
MASTER OF SCIENCE

Major Subject: Nuclear Engineering

Signatures have been redacted for privacy

---

Iowa State University  
Of Science and Technology  
Ames, Iowa

1961

## TABLE OF CONTENTS

	Page
INTRODUCTION	1
REVIEW OF LITERATURE	6
INVESTIGATION	8
EQUIPMENT AND MATERIAL	10
Radiation Source	10
Detector and Apparatus	10
Shielding	11
Absorbers	11
PROCEDURES	15
RESULTS AND DISCUSSION	20
CONCLUSIONS	39
LITERATURE CITED	41
ACKNOWLEDGMENTS	43
APPENDIX	44

## INTRODUCTION

Since the advent of nuclear power it has become necessary to find good radiation shielding material. Some of the desired properties for a nuclear reactor shield are (a) high density to minimize thickness, (b) high content of light elements for the degradation of the neutron flux, (c) high content of heavy elements for the degradation of gamma rays, (d) low cost, (e) ease of fabrication and installation, and (f) reasonable structural strength, including stability under irradiation and stability under hot, moist, or dry conditions. (1)

Light elements such as hydrogen and carbon are good neutron shields, but are ineffective as gamma ray shields, while in contrast, heavy elements such as lead are excellent gamma ray shields but poor neutron shields. Therefore, a good shielding material would be one that combines both the heavy and the light elements. Concrete is one of the few materials that meets these requirements. Concrete, a material consisting of inert aggregate bound together by a hardened cement paste, is a natural choice for a material for shielding stationary nuclear reactors. It is fairly effective in the attenuation of both neutron and gamma radiation escaping from the reactor system, has good structural properties and is not expensive. It is a material of excellent adaptability

in two respects: First, it can be molded with ease into any desired shape, and second, by varying the constituents, its shielding properties can be adapted to a wide range of requirements. (2)

Jaeger (2) also states that the required concrete thickness is determined by the gamma ray attenuation, and not by the neutron attenuation. The light elements present in the concrete moderate the neutrons so that the neutron flux is at a desirable level when the gamma rays have been reduced to a reasonable level.

The major property of the attenuation of gamma rays is the exponential decrease in the intensity of radiation as a homogeneous beam passes through a thin slab of material. If a beam of photons of flux intensity  $I$  strikes an absorber which has a thickness  $x$ , a number of atoms per unit volume  $n$ , and a collision cross section of  $\sigma$ , then the number of collisions made in a path length  $dx$  by photons passing through a unit cross section in a unit time is  $I\sigma ndx$ . Replacing  $\sigma n$  with the macroscopic linear absorption coefficient  $\mu$ , the relationship is then  $I\mu dx$ . If each photon involved in a collision is considered completely absorbed, then the number of collisions must equal the decrease in flux over the distance  $dx$ . Therefore, the differential equation

$$-dI = I\mu dx$$

is true. The solution of this equation when  $I_0$  is the

incident intensity is the well known absorption law

$$I = I_0 e^{-\mu x} .$$

The constant  $\mu$  can be determined by either theoretical or experimental means. (3)

The interaction of gamma rays with matter is described by three major processes; (a) photoelectric absorption, (b) Compton scattering, and (3) pair-production. The absorption coefficient depends on the properties of the absorbing material as well as the energy of the incident photon; therefore, no single formula or curve has been determined for all materials. Formulas have been derived for the probability of each of the above processes occurring as a function of energy. Therefore, the sum of each of the partial coefficients is the total absorption coefficient as a function of energy for a given material. (4)

The contribution of each process varies with the photon energy and the absorbing material. In the photoelectric effect all the energy is transferred to a bound electron which is ejected from the atom or molecule. Except in the heaviest elements photoelectric absorption is relatively unimportant for energies above 1 Mev. (4)

Instead of giving all its energy to a bound electron as in the above case the photon may give only part of its energy to either a bound or free electron and continue on an altered

path. This process is known as Compton scattering and occurs mainly at photon energies of 0.6 to 4.0 Mev. (4)

The pair-production process involves the creation of a positron-electron pair by the absorption of a photon. This process cannot take place at energies of less than 1.02 Mev. Therefore, it is important only at high gamma ray energies and for elements of high atomic number. (4)

The results from the evaluation of the absorption coefficients were compared with experimental results as reviewed by Davisson and Evans (5). The results indicate excellent agreement between theory and experiment.

To obtain valid experimental results and to be able to use the standard gamma ray attenuation equation, the following assumptions were made: (a) the incident beam was considered to be mono-energetic, i.e., 1.25 Mev., (b) the beam was considered to be collimated, i.e., no scattered radiation was scattered back into the beam, and (c) the absorbers were thin. With these assumptions in mind, the gamma ray attenuation equation is valid, and the absorption coefficients can be determined by measuring the beam intensity at various absorber thicknesses.

In calculation of the attenuation of gamma radiation, the buildup factor is normally given. This is the factor which is the ratio between the total gamma radiation contribution to the unscattered contribution. (3)

The determination of the buildup factor is usually accomplished by taking two measurements. First, a narrow beam attenuation is found using a collimated beam of monoenergetic gamma rays and a collimated detector. Then a broad beam attenuation is found using monoenergetic gamma rays without collimation. The ratio between the broad and the narrow beam attenuation is the buildup factor. (3)

Since a collimated beam was used in this study and no data was taken with a wide beam, the buildup factor for concrete was not determined. It, therefore, should be kept in mind that the results of this investigation should be multiplied by an appropriate buildup factor to determine the total contribution of the gamma radiation.



## REVIEW OF LITERATURE

Entrainment of a small amount of air in the cement paste has been found to improve considerably the durability of concrete and improve the resistance of the concrete to frost action. In certain areas of Kansas, Nebraska, Missouri, and Iowa natural coarse aggregates are scarce. Therefore, construction concrete is made using aggregate with a maximum size of  $3/8$  inch and containing a large amount of particles which pass the No. 4 sieve. This concrete contains about 2 to 4 percent air. The use of air-entraining agents increases the air content to 7 to 13 percent. It is the air content produced by the air-entraining agent that gives the concrete durability. Due to this entrained air the density of the concrete is decreased to some extent. (6)

As a rough approximation the ratio of the densities of two shielding materials can be related to the ratio of their absorption coefficients in the energy range of 1 to 3 Mev. Therefore, a concrete of less density would be less desirable and require a thicker shield. (7)

Heavy concrete has been used in conjunction with the shielding requirements of many nuclear reactors now in operation. The properties, composition, and cost of many of the well known heavy concretes have been reviewed by Snyder (7) and Hungerford (8). In most cases the densities of the

concrete is increased by replacing the standard aggregate by heavier aggregate, such as iron ore or iron fillings.

Price et al. (9) discusses in great detail the use of ordinary concrete as both a neutron and a gamma ray shield. They also state, as it has been stated before, that higher density concretes are better shielding materials for gamma rays. It was also stated in (9) that the variance of the cement to aggregate ratio has an effect on the neutron attenuation properties and that "leaner" mixes have an advantage over "rich" mixes. A water-cement ratio increase reduces the strength and density.

## INVESTIGATION

Since the compression strength and the workability depend directly upon the water-cement ratio, different water-cement ratios are used for different construction situations. Hence, a variation of water-cement ratios from 4 to 9 gallons of water per sack of cement was studied to see if there is any marked change in the gamma ray attenuation. Since the slump was controlled at 3 or 4 inches and the volume of water to coarse aggregate was held constant, the change in the water-cement ratio caused a change in the volume of cement and fine aggregate. This resulted in a decrease in the density as the water-cement ratio increased. Gamma ray attenuation varies mainly with the density; therefore, it is expected that the gamma ray attenuation should increase as the water-cement ratio increases.

Air-entrainment of concrete is used to reduce the effect of repeated freezing and thawing in temperate climates. Since a concrete shield for a nuclear reactor or other irradiation facility might be made of air-entrained concrete, an investigation of the gamma ray attenuation in air-entrained concrete was made to determine whether or not entrained air has any detrimental effects on the attenuation. The water cement-ratio was also varied in this investigation.

The study was conducted at only one energy level of incident gamma rays.

## EQUIPMENT AND MATERIAL

### Radiation Source

A cobalt-60 source of 2.1 curies was utilized in this study. This source is a special two-curie cobalt-60 irradiation facility located at Iowa State University of Science and Technology, Ames, Iowa. The source is located on a movable control rod which moves vertically along the axis of a 16-inch diameter lead cylinder. When the source is in the "up" position a collimated beam is produced horizontally. The beam is  $1/4$  inch in diameter at the edge of the lead cylinder. (10)

The cobalt-60 source emits two photons in cascade with energies of 1.17 Mev and 1.33 Mev. For this study an average energy of 1.25 Mev was used. Since cobalt-60 has a half life of 5.2 years, no correction for its decay was necessary.

### Detector and Apparatus

The detector which was used in the study was a NaI (Tl) crystal scintillation detector, model DS-5, manufactured by Nuclear of Chicago. The NaI (Tl) crystal was  $1\frac{1}{8}$  inch in diameter. The detector was operated at a 2500 volt potential.

The scaler used was a model 181A scaler manufactured by Nuclear of Chicago. The scaler was operated in conjunction with a model 1810 Radiation Analyzer also manufactured by

Nuclear of Chicago. The analyzer was set at a base level of 625 volts with a window width of 5 volts. The operating high voltage was 926 volts and the gain set at  $1/4$ . The analyzer had been calibrated with a standard cesium-137 source so that a base level of 625 volts would correspond to a 1.25 Mev gamma ray.

### Shielding

Several 2 by 4 by 8 inch lead brick were built up around the detector. These lead brick were used to reduce the scattering effect and the background counts. Also a wall of lead brick was used to hold the concrete absorbers in place. Figure 1 shows a drawing of the experimental set up.

### Absorbers

The absorbers used were 2 by 2 by 4 inch mortar brick. The composition of these brick was varied and is described in detail in the section on procedures. The chemical analysis of the components of the concrete was not obtained but Table 1 shows the published values for the normal components of Type I Portland cement, as found in Bauer (6).

The fine and coarse aggregate was Des Moines River, Boone, Iowa sand and gravel with dune sand added to fill the gaps in grading. The sand and gravel was assumed to be 100 percent  $\text{SiO}_2$  and was graded in accordance with ASTM specifications for concrete aggregate C33-54T. Table 2 shows the

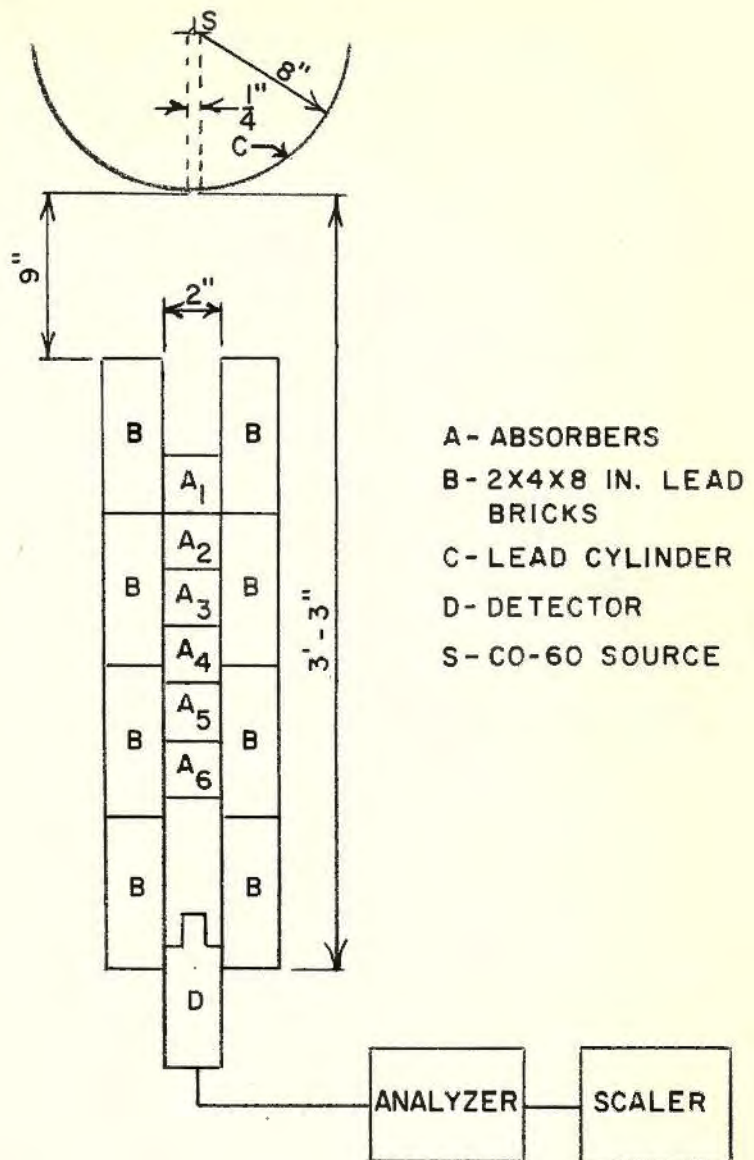


Figure 1. Experimental setup

particle distribution as determined by sieve analysis.

Tests on the unit weight, density, and water content of the aggregate was run in accordance with ASTM specifications. These values are listed in Table 3.

Table 1. Chemical composition of Portland cement Type I in percent weight

Compound	CaO	SiO <sub>2</sub>	Al <sub>2</sub> O <sub>3</sub>	MgO	SO <sub>3</sub>	Fe <sub>2</sub> O <sub>3</sub>
Percent	63.5	21.0	6.5	5.0	2.0	2.0

Table 2. Sieve analysis of sand and gravel

Screen size	Percent passed screen	
	Gravel	Sand
3/4 in.	100	
1/2 in.	95	
3/8 in.	55	100
No. 4	10	98
No. 8	2	90
No. 16		65
No. 30		42
No. 50		20
No. 100		5



Table 3. Properties of standard aggregate tests per ASTM specifications

Property	Sand	Gravel
Specific gravity	2.54	2.60
Unit weight (lb per cu ft)	114.2	104.4
Water content (percent)	0.75	0.09
Fineness modulus	2.80	

## PROCEDURES

The composition of the concrete brick was varied for this investigation. In all, twelve different mixes were used. In the first six mixes the water-cement ratio was varied from 4 to 9 gallons per sack. In the remaining six mixes the water-cement ratio was varied in the same manner as the former six except that an air-entraining agent was added to the mix to produce approximately 7.0% entrained air in the concrete. The air-entraining agent used was Vinsol Resin solution, which was a prepared mixture of one gram of Vinsol Resin crystals per ten ml of a 3.0% sodium hydroxide solution. The concrete mixes were proportioned using the American Concrete Institute method of proportioning. The amount of air-entraining agent used was determined by a graph in Troxell and Davis (11, p. 69). The composition by weight of the twelve mixes are shown in Table 4 and are labeled 1 through 12.

The procedure used for the mixing and casting of the brick was the same for all mixtures. The cement and the fine aggregate were mixed thoroughly by hand. The coarse aggregate was then added and mixed with a hand trowel. Finally the water was added slowly and mixed thoroughly with the cement and aggregate. The mixing continued for several minutes to insure a constant distribution of all components.

Table 4. Proportions of ingredients by weight in pounds

Batch	Cement	Water	Fine aggregate	Coarse aggregate	Air- entraining solution
1	4.70	1.66	4.69	6.38	0
2	3.74	1.66	5.43	6.38	0
3	3.12	1.66	5.94	6.38	0
4	2.68	1.66	6.27	6.38	0
5	2.35	1.66	6.55	6.38	0
6	2.08	1.66	6.77	6.38	0
7	4.16	1.49	4.96	6.38	7.0 Ml
8	3.33	1.49	5.32	6.38	4.8 Ml
9	2.77	1.49	5.79	6.38	3.6 Ml
10	2.38	1.49	6.13	6.38	2.9 Ml
11	2.08	1.49	6.36	6.38	2.3 Ml
12	1.85	1.49	6.55	6.38	1.8 Ml

For the air-entrained samples the Visol Resin solution was added to the water before it was mixed with the dry components.

Machined steel molds containing twenty-four 2 by 2 by 4 inch compartments were used for the forms. Batches of 12 brick each for the 12 mixes were cast. After the forms had been thoroughly greased they were filled about one-third full and rodded about 25 times. This procedure was repeated two more times to fill the mold. The remainder of the mortar was spread over the top and worked down with a trowel. The excess was removed leaving the mortar in the mold level with the top. The molds were then covered with wet burlap and

placed for two days in a 100% humidity moist room. The brick were then removed from the molds and placed under lime-saturated water for 26 more days.

The yield strength in compression was determined both 7 and 28 days after casting. Three bricks from each batch were tested at both 7 and 28 days. All compressive tests were made along the four inch length of the bricks with a hydraulic testing machine. The average compressive strength of the three bricks is reported in Table 5.

Table 5. Average compressive strength of concrete in psi

Batch no.	7 day test		28 day test	
	Theory <sup>a</sup>	Experiment	Theory <sup>b</sup>	Experiment
1	4400	3867	6000	4750
2	3500	3208	5000	4960
3	2800	2750	4000	3750
4	2200	2058	3200	3500
5	1800	1912	2500	2800
6	1400	1245	2000	2030
7	3800	3721	4800	4180
8	3000	3100	4000	4530
9	2400	2679	3200	3220
10	1900	1867	2600	2790
11	1500	1437	2000	2330
12	1200	1100	1600	1670

<sup>a</sup>Values are average values as reported in Ref. 12, p. 124.

<sup>b</sup>Values are average values as reported in Ref. 11, p. 107.

The experimental density for each of the 12 batches was determined by weighing each brick in water and in air. The theoretical density was determined from the mix proportioning. A comparison of the theoretical and experimental density gives the actual percent of air in the concrete. The average of these values for each batch is given in Table 6. The bricks were then used as absorbers and the counting rate was determined for 2 inch intervals of absorbers up to a total of 12 inches. The average count at each interval was corrected for background and normalized to the count rate at zero thickness. The normalized count versus absorber thickness was plotted on semi-log paper. The slope of the straight line obtained by this plot was determined by the least squares fit method applied to the equation of the line

$$\text{Activity} = ke^{-\mu x}$$

where  $\mu$  is the linear absorption coefficient in inches<sup>-1</sup>. Using the average experimental density obtained from the six bricks, the mass absorption coefficient,  $\mu/\rho$  was computed for each batch.

At the beginning of each day, the source was raised into position and clamped securely into place by "C clamps". Three five minute background counts were taken at the beginning of each batch. All data recorded in each batch was corrected for its respective background. Three five minute readings were taken starting with zero absorbers and every

Table 6. Density and air content of concrete blocks

Batch no.	Theory		Experiment	
	Unit weight pcf	% Air	Unit weight pcf	% Air
1	142.5	2.5	140.4	3.9
2	140.8	2.5	141.7	2.0
3	139.9	2.5	139.2	2.9
4	138.9	2.5	139.1	2.2
5	138.6	2.5	138.0	2.8
6	138.2	2.5	136.5	3.9
7	136.7	7.0	136.9	6.8
8	135.1	7.0	137.1	5.7
9	134.4	7.0	134.6	6.9
10	133.9	7.0	133.8	7.0
11	133.3	7.0	133.0	7.2
12	133.0	7.0	131.4	8.2

two inches thereafter until 12 inches of absorbers were placed between the source and the detector. The average of the three readings were used. Since a scintillation detector was used, no correction for counter dead time was required. Each batch required about two hours of counting time, therefore, only two batches could be run each day. Also it was impossible to maintain the same source geometry because the source was returned to its container at the end of each day. This explains the difference in the zero count rate of the different batches. At no time was the source moved while a run was being performed on a specific batch. The Appendix contains the data taken for all samples.

## RESULTS AND DISCUSSION

The results of the absorption coefficient tests are tabulated in Table 7. Figure 2 to Figure 7 show the absorption curves for the six different water-cement ratios. Both the air-entrained sample and the non-air-entrained sample for each water-cement ratio are plotted on the same axis. That is, Figure 2 shows the absorption curves for test number 1 and test number 7, and Figure 3 to Figure 7 show the absorption curves for both air and non-air-entrained samples of water-cement ratios of 5, 6, 7, 8, and 9 gallons per sack respectively. As an aid in evaluation of the results the density, linear absorption coefficients, and the compressive strengths for both 7 and 28 days were plotted versus the water-cement ratio of both the air and non-air-entrained samples. These plots are shown in Figures 8, 9, 10, and 11 respectively.

The plot of density versus the water-cement ratio, Figure 8, indicates three general characteristics; (a) a separation of the air and non-air-entrained curves, with the air-entrained sample being lower. This is to be expected because of the entrained air in the samples of the lower curve, (b) a general decrease in density as the water-cement ratio increased from 5 to 9 gallons per sack. This was also expected because more sand and less cement is present in the mixes of higher water-cement ratios. The specific gravity

Table 7. Experimental results of the mixtures tested

Batch no.	Water cement ratio gal/sack	Air content percent	Half thickness in.	Linear absorption coef. in. <sup>-1</sup>	Relaxation length cm.	Mass absorption coef. cm <sup>2</sup> /gm
1	4	3.9	2.34	0.296	8.58	0.0519
2	5	2.0	2.28	0.304	8.36	0.0527
3	6	2.9	2.28	0.304	8.36	0.0535
4	7	2.2	2.24	0.309	8.23	0.0545
5	8	2.8	2.24	0.309	8.23	0.0550
6	9	3.9	2.39	0.290	8.75	0.0522
7	4	6.8	2.22	0.312	8.15	0.0560
8	5	5.7	2.25	0.308	8.25	0.0552
9	6	6.9	2.25	0.308	8.25	0.0562
10	7	7.0	2.28	0.304	8.36	0.0559
11	8	7.2	2.31	0.300	8.46	0.0568
12	9	8.2	2.41	0.287	8.85	0.0538



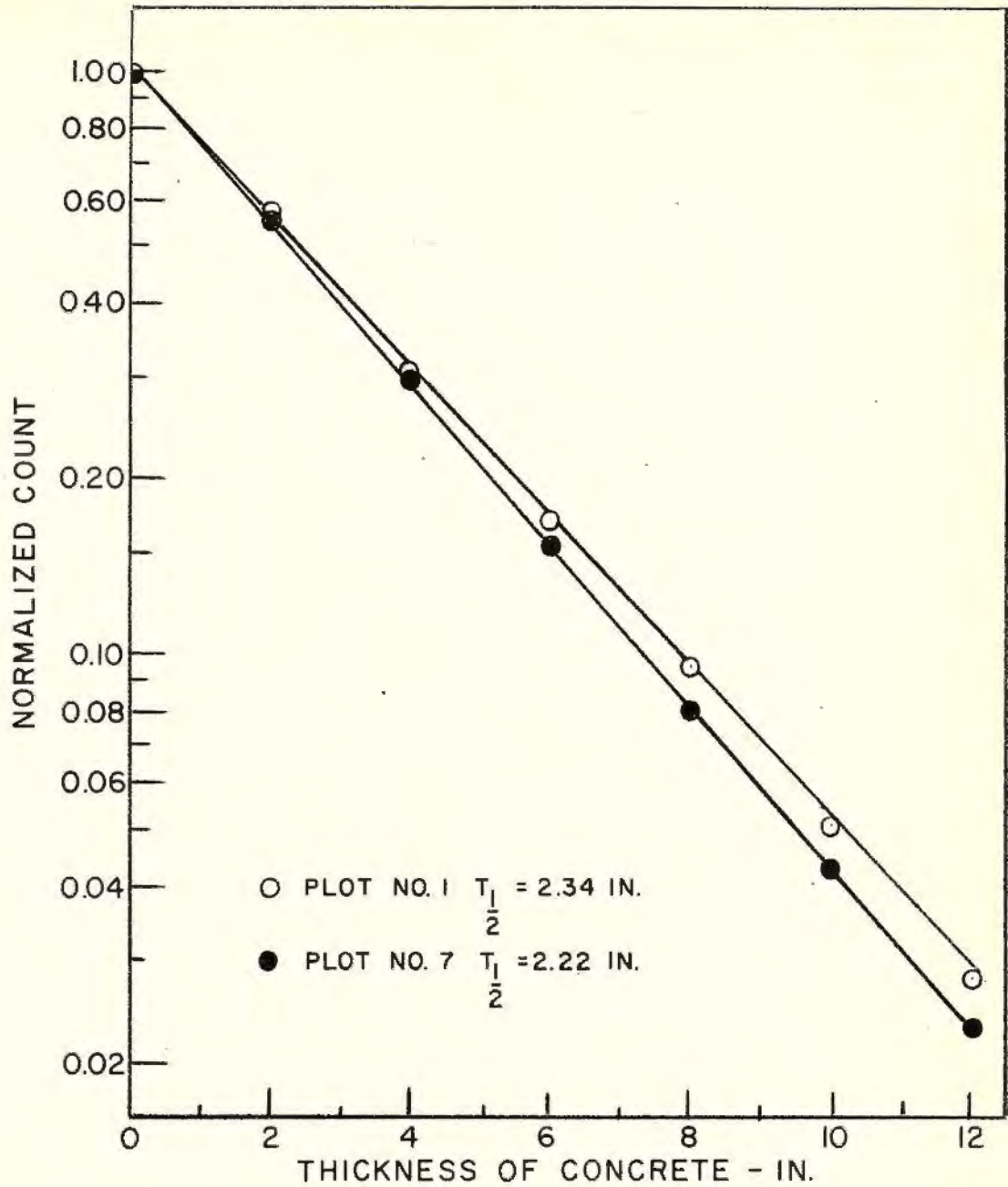


Figure 2. Absorption curve mixtures No. 1 and No. 7

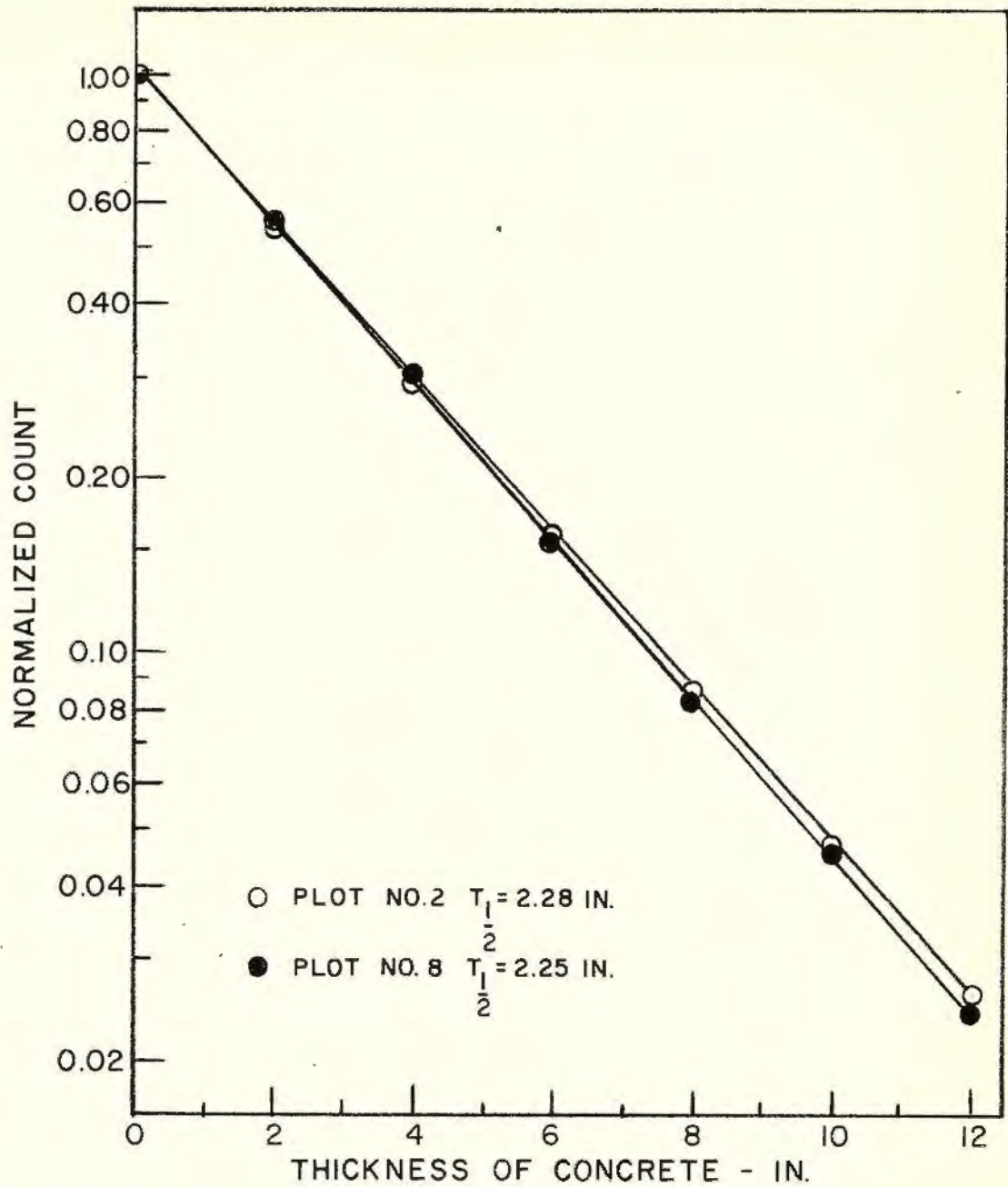


Figure 3. Absorption curve mixtures No. 2 and No. 8

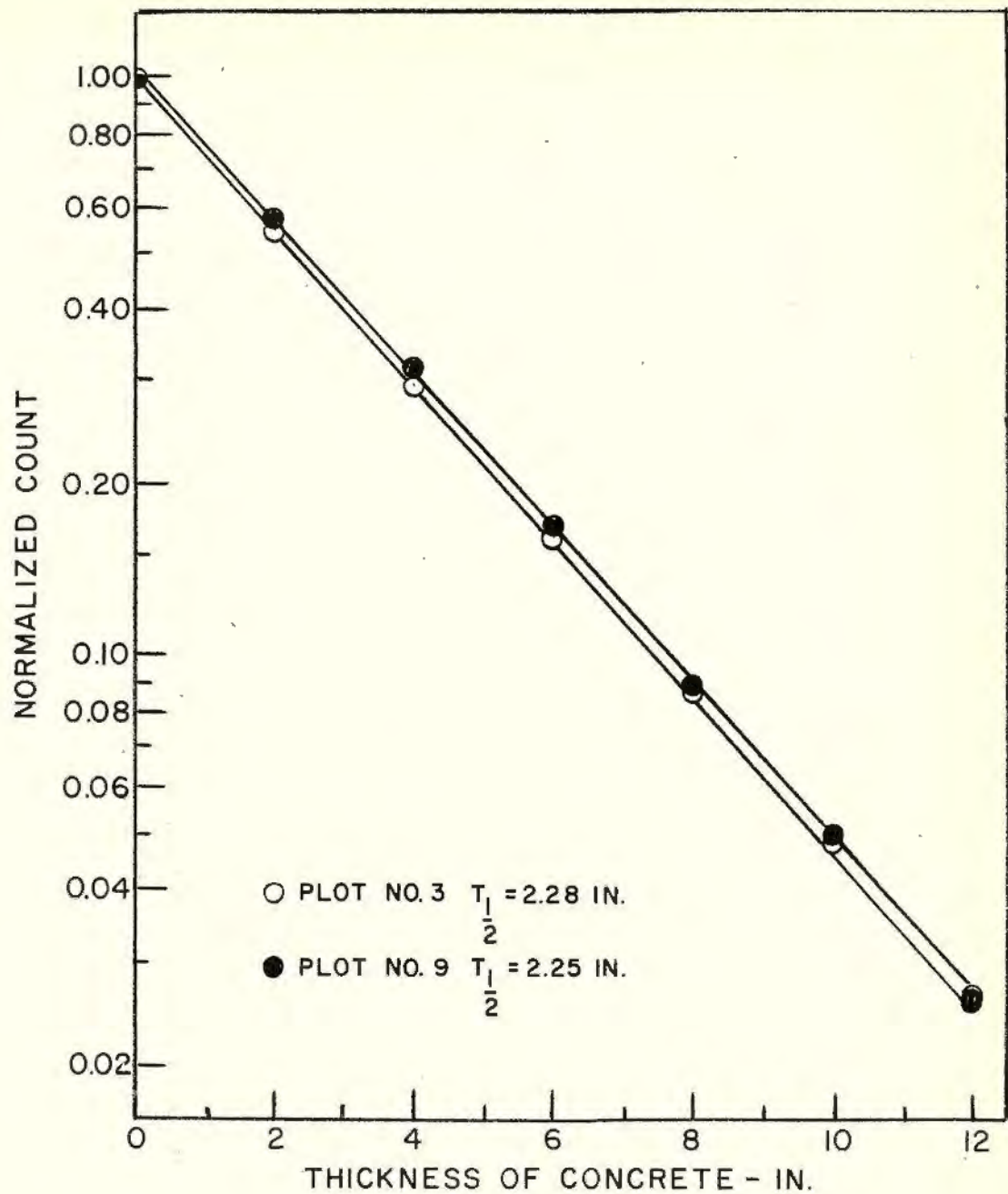


Figure 4. Absorption curve mixtures No. 3 and No. 9

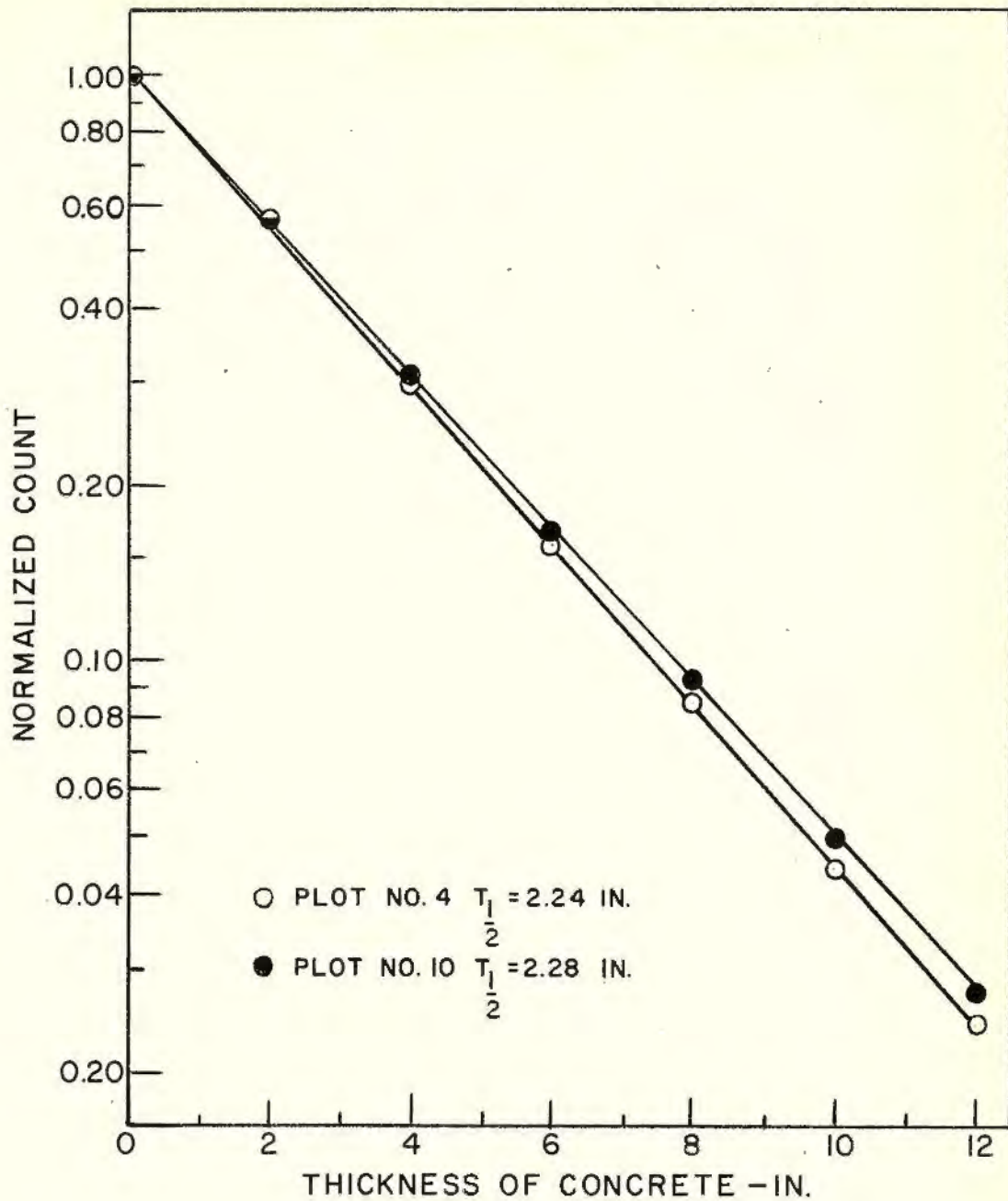


Figure 5. Absorption curve mixtures No. 4 and No. 10

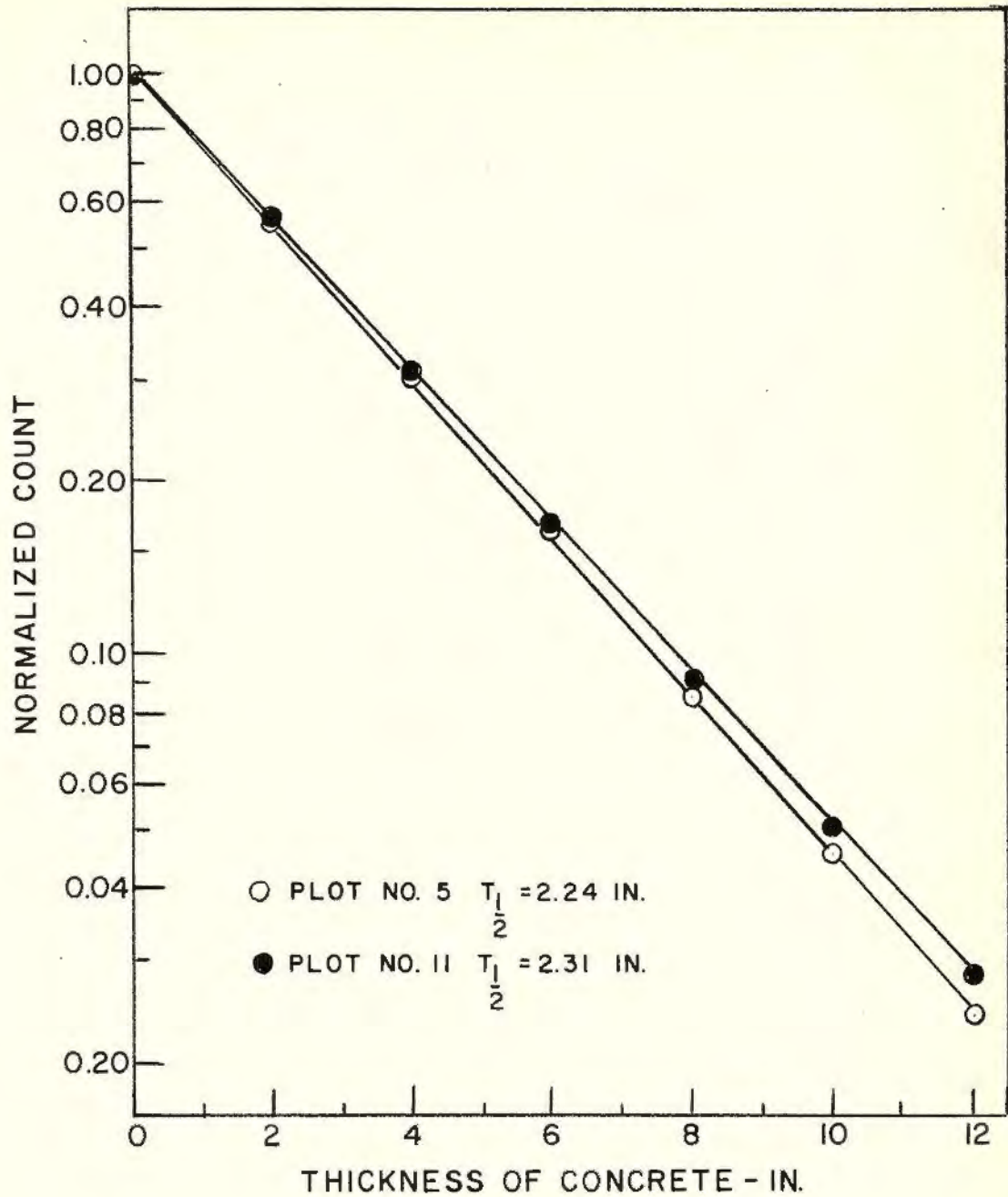


Figure 6. Absorption curve mixtures No. 5 and No. 11



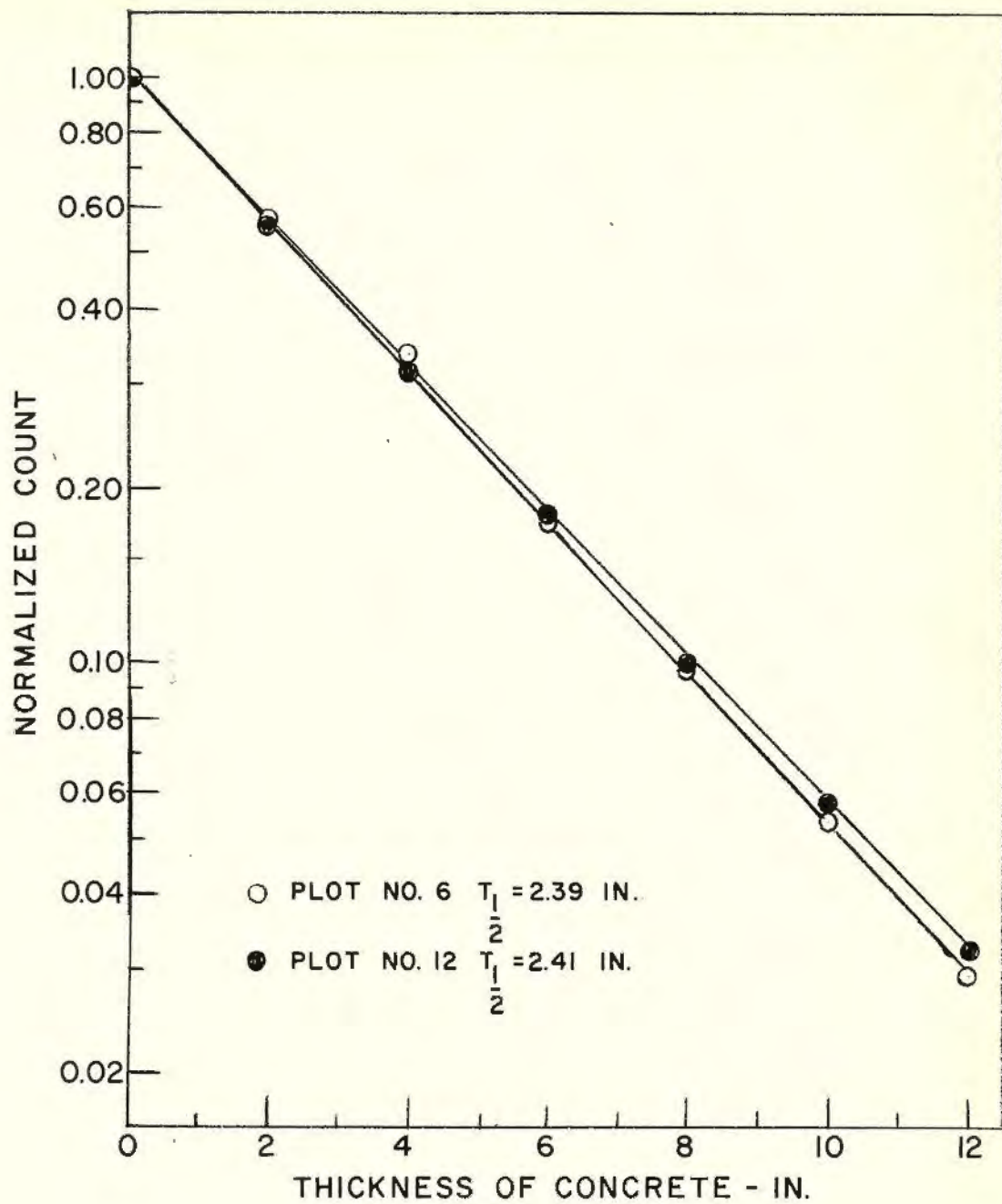


Figure 7. Absorption curve mixtures No. 6 and No. 12

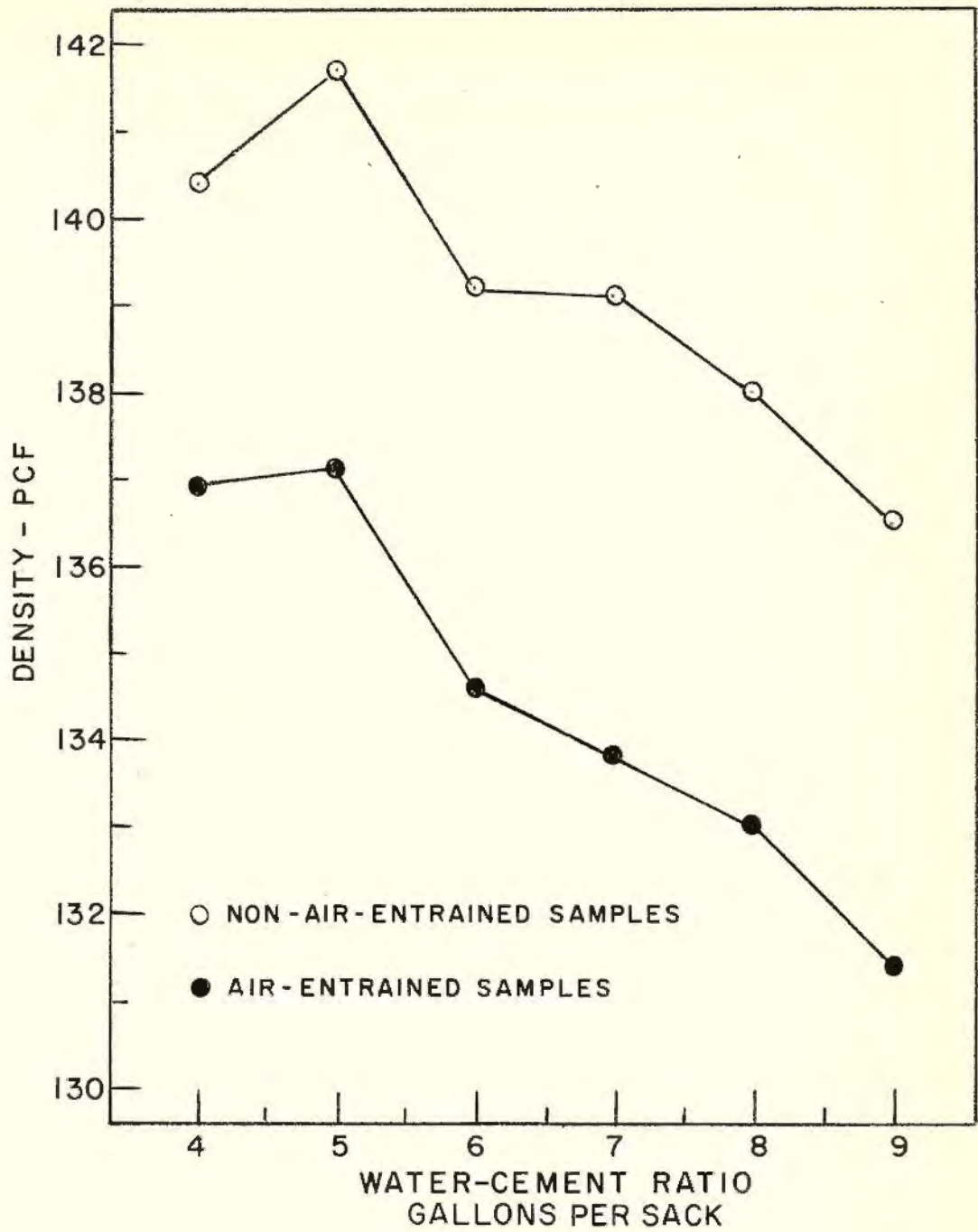


Figure 8. Density curves

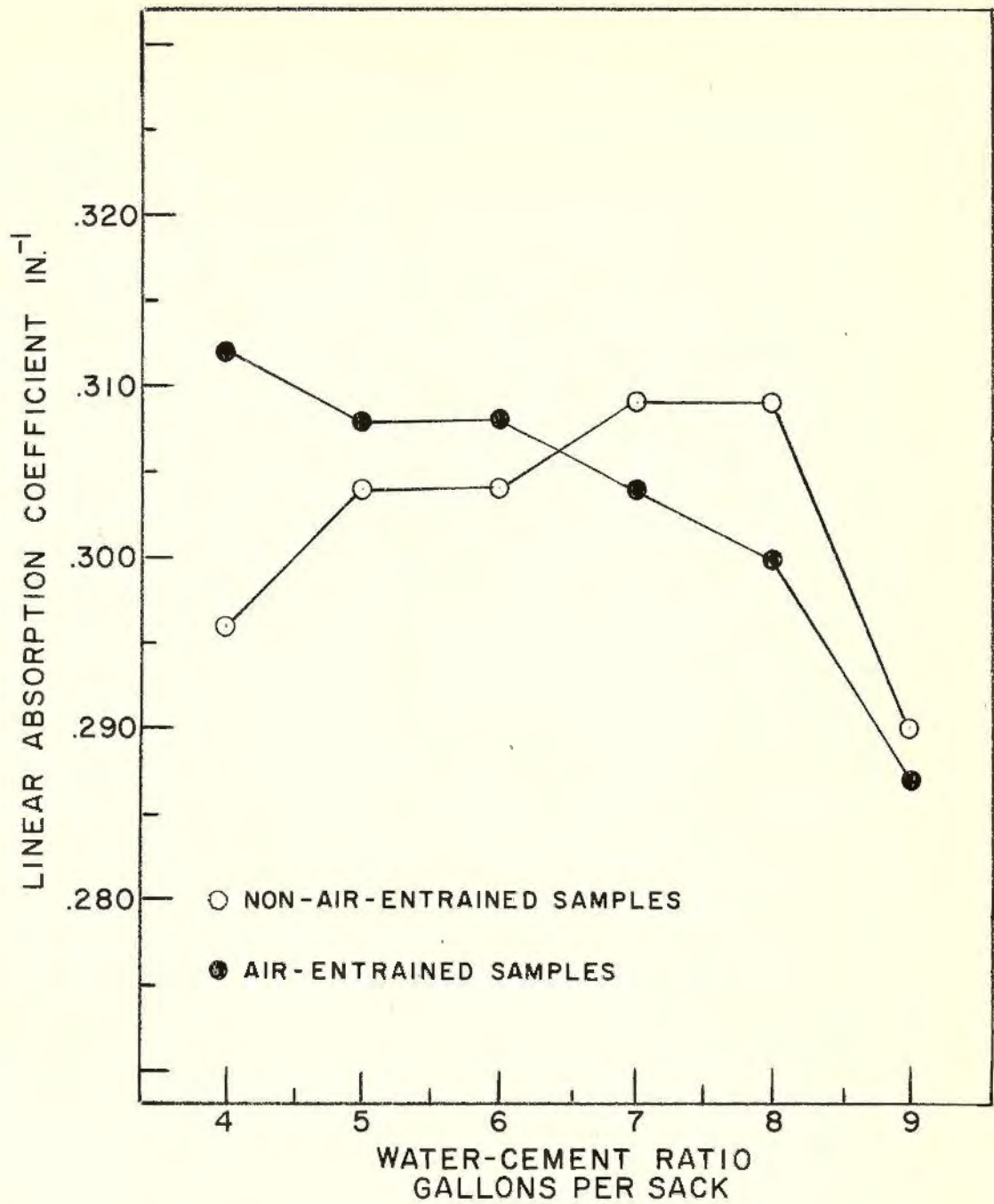


Figure 9. Linear absorption coefficient curve



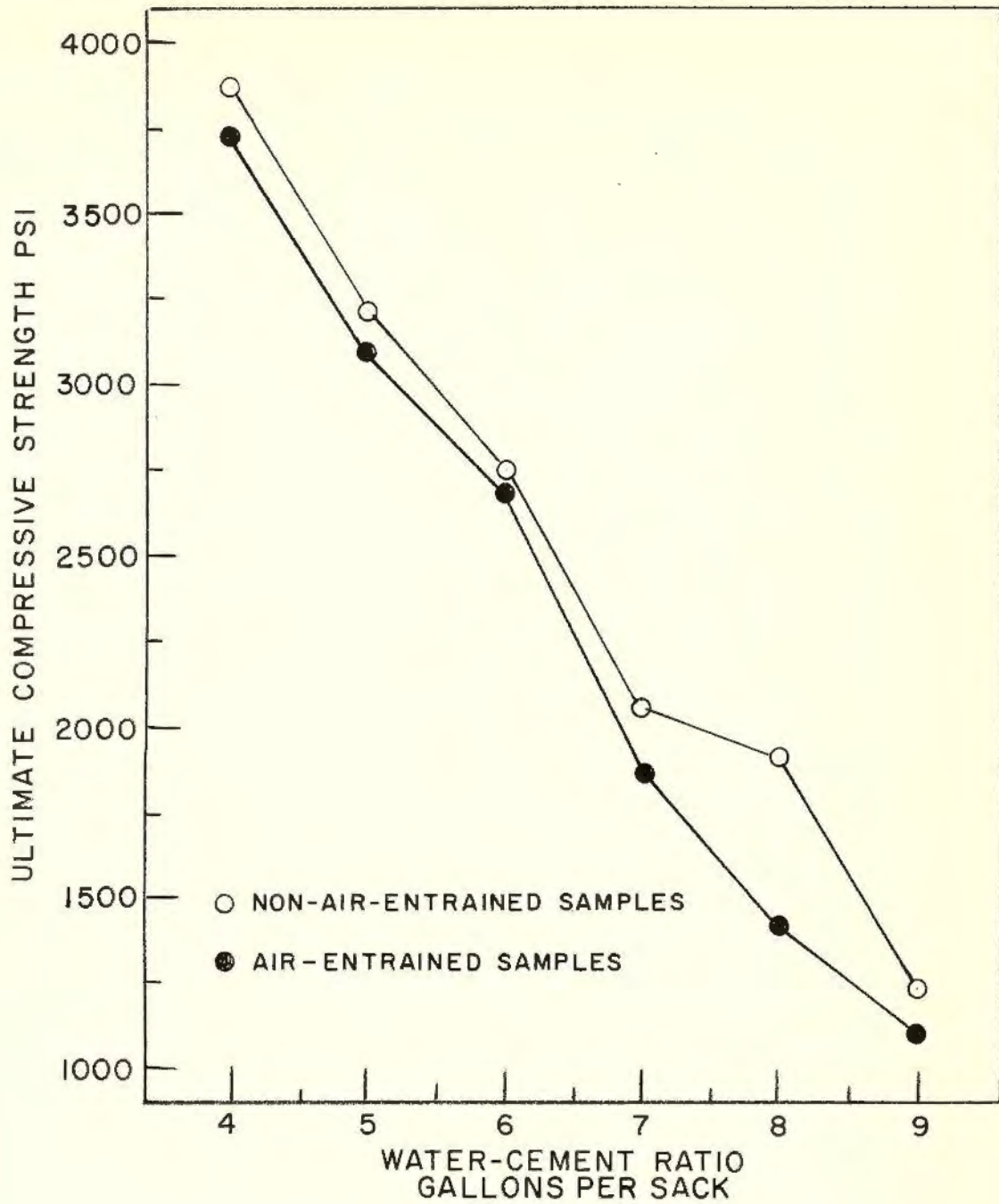


Figure 10. 7-day compressive strength curves

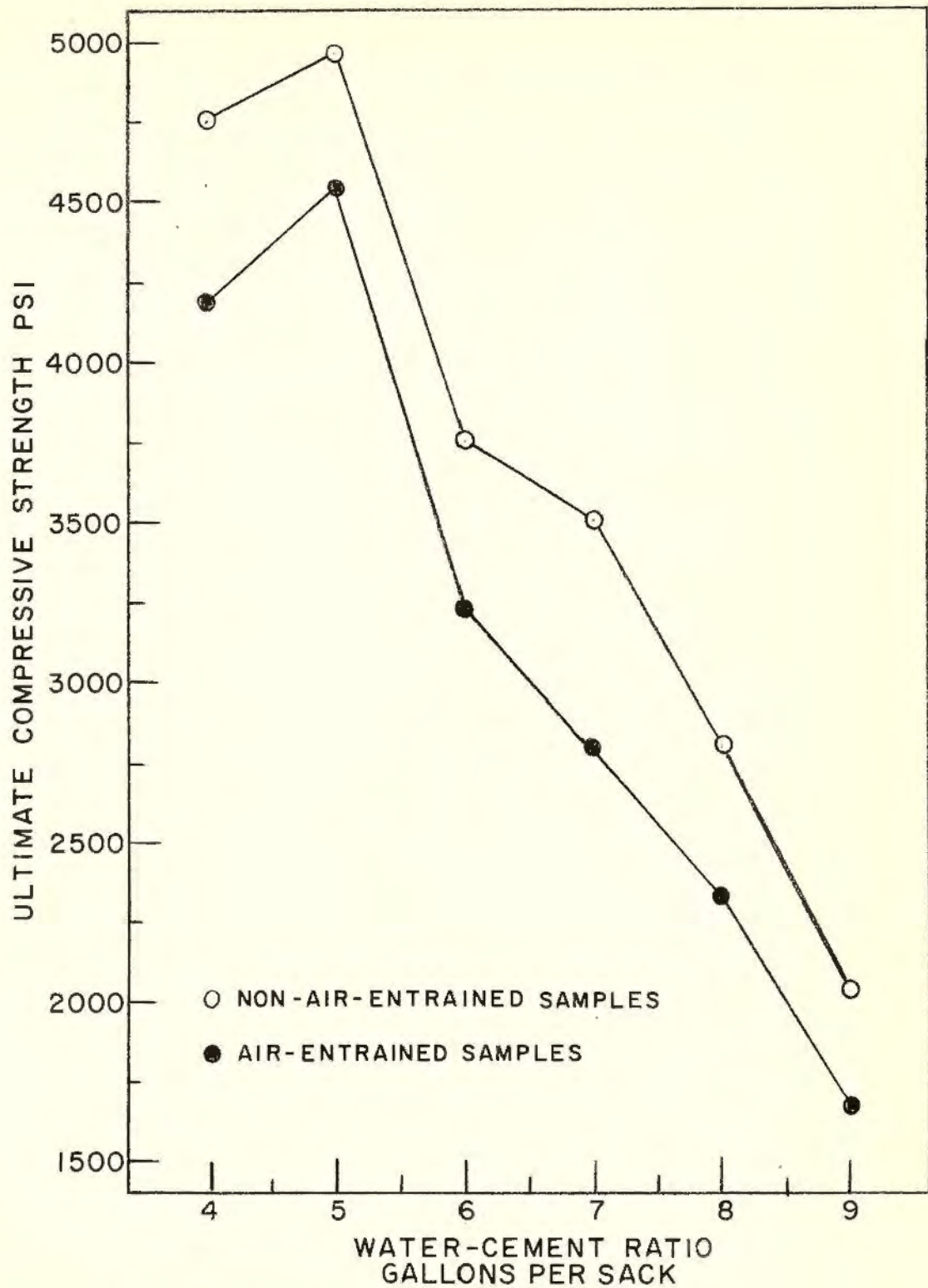


Figure 11. 28-day compressive strength curves

of sand is 2.54 compared to 3.2 for the cement, (c) it should be noted that at the water-cement ratios of 4 and 9 gallons per sack this does not occur. The density is much less than that at adjacent points, which is not what would be expected. This phenomenon will be discussed later in this section.

The plot of the linear absorption coefficient versus the water-cement ratio for the non-air-entrained mixes, Figure 9, shows a marked decrease in the coefficient at water-cement ratios of 4 and 9 gallons per sack. This decrease is at the same water-cement ratios as mentioned in the preceding paragraph. Also an examination of Figure 11, the 28 day compressive strength versus the water-cement ratio, shows a decrease in strength at the same water-cement ratios. This indicates that the samples in question were probably too porous. A recheck of Table 6 shows that the air content of these samples was 3.9% where the average of the other four samples was about 2.0%. The explanation for this increase in air content and porosity is that (a) at the water-cement ratio of 4 gallons per sack the mix was extremely "harsh" and more air was trapped in the mix due to the extra rodding required to make the mix workable, (b) at the water-cement ratio of 9 gallons per sack the mix was quite fluid because the amount of cement was low. This would cause a less dense mixture. Therefore, if the samples at water-cement ratios of 4 and 9 were neglected, the plot of the linear absorption coefficient

versus the water-cement ratio for the non-air-entrained samples shows relatively little change for the different water-cement ratios. The compressive strength for both 7 and 28 days shows a decrease as the water-cement ratio increases except at the lowest ratio as was noted previously. Also the air-entrained sample has less compressive strength than was expected. Table 5 shows a comparison of the theoretical and experimental compressive strength.

Since the chemical analysis of the ingredients was not available, no exact comparison of the theoretical and experimental values can be made. In order to obtain some comparison between theory and experiment, the mass absorption coefficients were computed for all twelve mixtures using the average published composition as reported in Table 1. The theoretical mass absorption coefficients were computed for an incident photon energy of 1.25 Mev.

The linear absorption coefficient for the elements that appear in the compounds listed in Table 1 were computed by using formulas found in Siri (13). Since the total linear absorption coefficient is made up of three partial linear absorption coefficients, the partial coefficients were computed for each element using the following equations:

(a) Photoelectric effect,

$$\tau = 4.07 \tau_{pb} \frac{\rho z^4}{A} \times 10^{-7}$$

(b) Compton effect,

$$\sigma = 0.224 \sigma_{pb} \frac{\rho z}{A}$$

(c) Pair production,

$$\kappa = 2.725 \kappa_{pb} \frac{z^2}{A} \times 10^{-3}.$$

The values for lead were obtained from curves as  $\tau_{pb} = 0.14$ ,  $\sigma_{pb} = 0.51$ , and  $\kappa_{pb} = 0.002$ . The total linear absorption coefficient is the sum of the partial coefficient,  $\mu = \tau + \sigma + \kappa$ . The mass absorption coefficients were obtained by dividing the above results by the density of the element in question. The densities were the standard density at 15°C as reported in Nucleonics (14). The theoretical mass absorption coefficients for the elements needed are shown in Table 8. As a check on these values, the values listed by Hungerford (8) at several energy levels were plotted and the value at 1.25 Mev is also presented in Table 8.

The mass absorption coefficient for a compound or mixture was determined by a weight fraction summation, that is

$$\mu/\rho = f_1 \frac{\mu_1}{\rho_1} + f_2 \frac{\mu_2}{\rho_2} + \dots$$

where  $f_1$ ,  $f_2$ , etc. are the fractional weight percentages of the elements present. As an example, the mass absorption

coefficient for  $\text{SO}_3$  was obtained, using the values for sulfur and oxygen found in Table 8, as

$$\mu/\rho = 32/80 (.0570) + 48/80 (.0577) = 0.0574$$

The values computed for all the compounds are listed in Table 9.

Table 8. Mass absorption coefficients

Element	$\mu/\rho \text{ cm}^2/\text{gm}$	
	Hungerford's values	Theoretical values
Al	0.0553	0.0550
Ca	0.0575	0.0574
Fe	0.0538	0.0533
H	0.1125	0.1140
Mg	0.0565	0.0572
O	0.0574	0.0577
Si	0.0573	0.0573
S	0.0570	0.0570

Table 9. Mass absorption coefficients of compounds

Compounds	$\mu/\rho \text{ cm}^2/\text{gm}$
$\text{Al}_2\text{O}_3$	0.0563
$\text{CaO}$	0.0575
$\text{Fe}_2\text{O}_3$	0.0550
$\text{H}_2\text{O}$	0.0640
$\text{MgO}$	0.0574
$\text{SO}_3$	0.0574
$\text{SiO}_2$	0.0576

The theoretical mass absorption coefficient for Portland cement Type I was found in the same manner, using Table 1 for the percent fraction of each compound and Table 9 for the mass absorption coefficient of the compound. The theoretical mass absorption coefficient for cement is

$$\begin{aligned}\mu/\rho &= .0575 \times .635 + .0576 \times .210 + .0563 \times .065 \\ &\quad .0574 \times .050 + .0574 \times .020 + .0550 \times .020 \\ &= 0.0574.\end{aligned}$$

Table 10 shows the mass absorption coefficient of the components used in the concrete mixes.

Table 10. Mass absorption coefficient of concrete ingredients

Material	$\mu/\rho$ cm <sup>2</sup> /gm
Cement	0.0574
Sand	0.0576
Gravel	0.0576
Water	0.0640

Using the above figures and the weight proportions given in Table 4 for cement, aggregate and water, the mass absorption coefficients for all twelve mixes were computed. These theoretical values are compared with the experimentally obtained values in Table 11.

Since the percentage difference for the air-entrained samples are less than that for the non-air-entrained samples, it could be assumed that the air-entrained data are more accurate. This is also true in the plot of the linear coefficient which was discussed earlier. The experimental results indicate that there is little change in the absorption coefficient due to a change in water-cement ratio. This is true because as the water-cement ratio increases the weight of cement decreases while the weight of sand increases proportionately. Since there is little difference between the absorption coefficient of sand and cement, the change in the absorption coefficient is slight. The mass absorption coefficient for the air-entrained concrete is higher than that for the non-air-entrained concrete. This is true because the linear coefficient is primarily the same but the density of the air-entrained concrete is less. Table 11 shows that the percentage differences in  $\mu/\rho$  for all mixes is less than 10 percent; therefore, the experimental results do agree within reason to the results which were predicted by the theoretical analysis.



Table 11. Theoretical and experimental mass absorption coefficients

Water cement ratio	$\mu/\rho$ cm <sup>2</sup> /gm					
	Non-air-entrained			Air-entrained		
	Theory	Experiment	% error	Theory	Experiment	% error
4	0.0576	0.0519	9.9	0.0548	0.0560	2.2
5	0.0576	0.0527	8.5	0.0548	0.0552	0.7
6	0.0576	0.0535	7.1	0.0548	0.0562	2.5
7	0.0576	0.0545	5.4	0.0548	0.0559	2.0
8	0.0576	0.0550	4.5	0.0548	0.0568	3.6
9	0.0576	0.0522	9.4	0.0548	0.0538	1.8

## CONCLUSIONS

The results of the tests of the gamma ray shielding properties of concrete with varying water-cement ratios and air-entrainment indicate that the following conclusions may be drawn within the range of water-cement ratios and concrete composition studied in this investigation:

1. The variation of the water-cement ratio for a standard non-air-entrained mixture produced little change in the linear absorption coefficient.
2. An increase of the water-cement ratio from 5 to 8 gallons per sack for a standard non-air-entrained mixture produced an increase in the mass absorption coefficient of 4.5 percent.
3. The variation of the water-cement ratio for an air-entrained mixture produced little change in the linear absorption coefficient.
4. An increase of the water-cement ratio from 5 to 8 gallons per sack for an air-entrained mixture produced an increase in the mass absorption coefficient of 3.0 percent.
5. The linear absorption coefficient is about 1.0 percent less for an air-entrained mixture than for a standard non-air-entrained mixture.

6. The mass absorption coefficient is about 4.0 percent greater for an air-entrained mixture than for a standard non-air-entrained mixture.
7. Since the changes are all quite small, it can be assumed that generally the gamma ray absorption properties are not changed considerably with air entrainment up to 7.0 percent.

## LITERATURE CITED

1. Gallaher, R. B. and Kitzes, A. S. Summary report on Portland cement concretes for shielding. U. S. Atomic Energy Commission Report ORNL-1414 [Oak Ridge National Lab., Tenn.] March, 1953.
2. Jaeger, T. Concrete--the convenient reactor shielding. Atomic World 9: 416-18. 1958.
3. Cowden, Jack. Spectral study of the attenuation of gamma radiation. Unpublished M.S. Thesis. Ames, Iowa, Library, Iowa State University of Science and Technology. 1959.
4. Friedlander, G. and Kennedy, J. W. Nuclear and radio-chemistry. New York, N. Y., John Wiley and Sons, Inc. 1957.
5. Davisson, C. M. and Evans, R. D. Gamma ray absorption coefficients. Review of Modern Physics 24: 79-107. 1952.
6. Bauer, E. E. Plain concrete. 3rd ed. New York, N. Y., McGraw-Hill Book Co., Inc. 1949.
7. Snyder, M. J. Cement and concretes. In Reactor Handbook, Vol. 3, Chapt. 1.8. U. S. Atomic Energy Commission, Technical Information Service. 1955.
8. Hungerford, H. E. Shielding materials. In Reactor Handbook, Vol. 1, Chapt. 2.9. U. S. Atomic Energy Commission, Technical Information Service. 1955.
9. Price, Horton, and Spinney. Radiation shielding. New York, N. Y., Pergamon Press. 1957.
10. McDermott, A. M. An irradiation facility with a two-curie cobalt-60 source. Unpublished M.S. Thesis. Ames, Iowa, Library, Iowa State University of Science and Technology. 1958.
11. Troxell, G. E. and Davis, H. E. Composition and properties of concrete. New York, N. Y., McGraw-Hill Book Co., Inc. 1956.

12. U. S. Department of the Army. Construction materials and engineer computations and layout, U. S. Dept. Army R.O.T.C. Manual 145-5-1. Washington, D. C., Author. 1956.
13. Siri, William, ed. Handbook of radioactive and tracer methodology. Dayton, Ohio, U.S.A.F. Material Command, Wright Patterson AFB. 1948.
14. Reference data manual. Nucleonics. 18, No. 11: 147-210. Nov. 1960.

## ACKNOWLEDGMENTS

This study was conducted as a part of the graduate program in Nuclear Engineering with a minor in Nuclear Science. Participation in this course of study was sponsored by the United States Army, Corps of Engineers.

The author wishes to express appreciation to Dr. Glenn Murphy for the guidance, encouragement, and assistance he gave during this study.

The author also wishes to thank Professor Stephen Chamberlin of the Department of Theoretical and Applied Mechanics for his helpfulness with the equipment used in casting the mortar specimens.

Thanks are also extended to Mr. Richard Danofsky for his help in setting up the radiation equipment for this study.

## APPENDIX

Table 12. Compression test data

Batch no.	7 day test: 7 Mar. 61				28 day test: 28 Mar. 61			
	Ultimate strength psi				Ultimate strength psi			
	Test	Test	Test	Av.	Test	Test	Test	Av.
	No.1	No.2	No.3		No.1	No.2	No.3	
1	4200	3900	3500	3867	5300	4150	4800	4750
2	3237	3287	3100	3208	4925	4450	5287	4960
3	2687	2987	2575	2750	4125	3275	3850	3750
4	2225	1775	2175	2058	3425	3525	3550	3500
5	1962	2025	1750	1912	2864	2687	2850	2800
6	1137	1337	1262	1245	2125	1950	2025	2030
7	3100	4025	4037	3721	3175	5465	3900	4180
8	3300	2837	3162	3100	4100	5000	4500	4530
9	2762	2600	2675	2679	3125	3600	2935	3220
10	1837	1762	2000	1867	3163	2633	2563	2790
11	1337	1600	1312	1437	2182	2407	2400	2330
12	1087	1075	1137	1100	1850	1512	1650	1670



Table 13. Density test data (Date: 29 May 61)

Batch no.	Brick no.	Wt. in air gm.	Wt. in water gm.	Density pcf
1	1	603	337	140.9
	2	601	334	140.2
	3	599	332	139.8
	4	599	334	140.9
	5	600	334	140.2
	6	589	327	140.2
			Av.	<u>140.4</u>
2	1	612	343	141.7
	2	590	327	139.8
	3	609	340	141.0
	4	597	331	139.8
	5	600	344	146.0
	6	609	341	141.7
			Av.	<u>141.7</u>
3	1	596	330	139.8
	2	605	336	139.2
	3	596	328	138.5
	4	602	332	139.2
	5	604	335	139.8
	6	596	328	138.5
			Av.	<u>139.2</u>
4	1	589	322	137.3
	2	603	334	139.6
	3	606	334	138.9
	4	599	330	138.5
	5	600	333	140.5
	6	605	335	139.6
			Av.	<u>139.1</u>
5	1	590	326	138.9
	2	583	318	137.2
	3	594	324	137.2
	4	601	328	137.2
	5	604	333	138.9
	6	600	331	138.9
			Av.	<u>138.0</u>

Table 13 (Continued).

Batch no.	Brick no.	Wt. in air gm..	Wt. in water gm.	Density pcf
6	1	578	314	136.5
	2	583	321	138.3
	3	571	307	134.6
	4	585	319	137.0
	5	574	312	136.5
	6	576	312	<u>135.9</u>
				Av. <u>136.5</u>
7	1	609	331	136.9
	2	610	332	136.9
	3	610	330	131.3
	4	615	336	137.4
	5	607	331	137.4
	6	607	329	<u>136.3</u>
				Av. <u>136.9</u>
8	1	600	327	137.1
	2	609	332	137.1
	3	612	336	138.4
	4	619	338	137.1
	5	598	323	135.8
	6	620	338	<u>137.1</u>
				Av. <u>137.1</u>
9	1	590	319	135.8
	2	580	309	133.4
	3	591	317	134.6
	4	569	306	134.6
	5	577	312	135.8
	6	572	304	<u>133.4</u>
				Av. <u>134.6</u>
10	1	583	312	134.0
	2	573	303	132.1
	3	592	317	134.0
	4	572	307	134.6
	5	581	311	134.0
	6	570	305	<u>134.0</u>
				Av. <u>133.8</u>

Table 13 (Continued).

Batch no.	Brick no.	Wt. in air gm.	Wt. in water gm.	Density pcf
11	1	587	314	134.0
	2	578	306	133.0
	3	549	291	133.0
	4	574	306	133.4
	5	570	300	134.0
	6	559	292	<u>130.6</u>
			Av.	133.0
12	1	582	309	132.8
	2	567	299	132.0
	3	574	302	131.3
	4	568	296	130.2
	5	569	299	131.3
	6	571	299	<u>131.0</u>
			Av.	131.4

Table 14. Counting data

Batch no.	Thick- ness in.	Count No. 1	Count No. 2	Count No. 3	Ave. count	Ave. rate	Corr. rate	Normalized rate			
1	Back-ground	326	852	811	827	29	165	6			
	0	379,355	378,821	378,737	378,971	616	75,794	123	75,629	129	1.000
	2	215,693	215,621	216,658	215,991	466	43,198	93	43,033	99	0.569
	4	116,521	116,662	116,389	116,524	342	23,305	68	23,140	74	0.306
	6	64,928	65,425	64,971	65,108	256	13,022	51	12,857	57	0.170
	8	36,021	36,195	36,199	36,138	191	7,228	38	7,063	44	0.095
	10	19,910	20,204	20,320	20,217	142	4,043	28	3,878	34	0.051
	12	11,536	11,434	11,602	11,524	107	2,305	21	2,140	27	0.028
2	Back-ground	914	872	881	889	30	178	6			
	0	382,243	383,572	383,759	383,191	620	76,638	124	76,460	130	1.000
	2	203,871	208,109	207,901	208,293	458	41,658	92	41,480	98	0.542
	4	111,507	111,745	111,957	111,736	334	22,347	67	22,169	73	0.290
	6	60,359	60,835	60,689	60,628	247	12,126	49	11,948	55	0.156
	8	33,810	33,900	33,664	33,791	184	6,758	37	6,589	43	0.086
	10	18,655	18,927	19,017	18,866	137	3,773	27	3,595	33	0.047
	12	10,765	10,697	10,762	10,741	104	2,148	21	1,970	27	0.026
3	Back-ground	995	983	941	973	31	195	6			
	0	431,979	432,538	434,502	433,006	660	86,601	132	86,406	138	1.000
	2	235,314	234,767	235,324	235,135	486	47,027	97	46,832	103	0.543
	4	127,725	126,627	126,851	127,068	357	25,414	71	25,219	77	0.292
	6	70,145	69,947	69,997	69,997	265	13,999	53	13,804	59	0.160
	8	38,407	38,558	38,457	38,474	196	7,695	39	7,500	45	0.087
	10	21,962	21,401	21,637	21,667	147	4,333	29	4,138	35	0.048
	12	12,208	12,357	12,255	12,273	111	2,455	22	2,260	28	0.026

Table 14 (Continued).

Batch no.	Thick- ness in.	Count No. 1	Count No. 2	Count No. 3	Ave. count		Ave. rate		Corr. rate	Normalized rate
4	Back- ground	1,020	1,104	1,117	1,093	33	219	7		
	0	476,239	482,352	490,813	483,135	696	96,627	139	96,408	146 1.000
	2	271,152	273,375	274,522	273,016	524	54,603	105	54,384	112 0.564
	4	143,749	144,627	144,748	144,375	382	28,875	76	28,656	83 0.297
	6	77,245	77,573	77,387	77,401	279	15,480	56	15,261	63 0.158
	8	41,509	41,727	41,550	41,599	204	8,320	41	8,101	48 0.084
	10	22,366	22,434	22,246	22,349	150	4,470	30	4,251	37 0.044
	12	12,510	12,668	12,524	12,567	112	2,513	22	2,294	29 0.024
5	Back- ground	1,036	1,058	1,049	1,048	32	210	6		
	0	503,578	509,276	516,750	509,868	715	101,974	143	101,764	149 1.000
	2	283,481	283,810	284,737	284,009	535	56,802	107	56,592	113 0.556
	4	153,157	154,245	153,633	153,678	392	30,736	78	30,526	84 0.300
	6	83,535	83,013	83,826	83,458	278	16,692	56	16,482	62 0.162
	8	43,755	43,730	43,962	43,816	210	8,763	42	8,553	48 0.084
	10	24,090	23,885	24,194	24,056	155	4,811	31	4,601	37 0.045
	12	13,178	13,073	13,252	13,168	115	2,634	23	2,424	29 0.024
6	Back- ground	917	915	921	918	30	184	6		
	0	396,223	400,414	409,219	401,952	635	80,390	127	80,206	133 1.000
	2	230,906	230,825	231,951	231,231	481	46,246	96	46,062	102 0.575
	4	125,449	126,076	125,914	125,813	355	25,163	71	24,979	77 0.336
	6	70,173	70,707	70,007	70,296	266	14,059	53	13,875	59 0.173
	8	39,286	39,703	40,077	39,689	199	7,938	40	7,754	46 0.097
	10	21,841	22,368	22,289	22,166	149	4,433	30	4,249	36 0.053
	12	12,566	12,586	12,630	12,594	112	2,519	22	2,335	28 0.029

Table 14 (Continued).

Batch no.	Thick- ness in.	Count No. 1	Count No. 2	Count No. 3	Ave. count	Ave. rate	Corr. rate	Normalized rate			
7	Back-ground	920	918	925	921	30	184	6			
	0	418,318	422,123	426,267	422,236	650	84,447	130	84,263	136	1.000
	2	233,255	233,178	234,939	233,757	485	46,751	97	46,567	103	0.554
	4	123,838	123,995	123,878	123,904	352	24,781	70	24,597	76	0.292
	6	65,183	65,002	65,136	65,107	256	13,021	51	12,837	57	0.152
	8	34,758	34,604	34,695	34,686	187	6,937	37	6,753	43	0.080
	10	18,947	19,094	18,987	19,009	138	3,802	28	3,618	34	0.043
	12	10,454	10,427	10,582	10,488	105	2,098	21	1,914	27	0.023
8	Back-ground	947	921	953	940	31	188	6			
	0	408,772	410,938	419,134	412,948	645	82,589	129	82,401	135	1.000
	2	228,973	229,913	231,875	230,254	481	46,051	96	45,863	102	0.556
	4	124,326	123,806	124,570	124,234	354	24,847	71	24,659	77	0.299
	6	64,594	64,547	65,254	64,570	255	12,914	51	12,726	57	0.155
	8	35,084	35,272	35,143	35,166	188	7,033	38	6,845	44	0.083
	10	19,408	19,168	19,516	19,364	139	3,873	28	3,685	34	0.045
	12	10,878	10,888	10,982	10,913	105	2,183	21	1,995	27	0.024
9	Back-ground	1,140	1,042	1,171	1,134	34	227	7			
	0	549,163	557,911	565,829	557,634	746	111,527	149	111,300	156	1.000
	2	319,479	320,007	323,501	320,996	570	64,199	114	63,972	121	0.574
	4	177,798	178,207	177,863	177,956	423	35,591	85	35,364	92	0.317
	6	94,489	94,406	94,585	94,493	308	18,899	62	18,672	69	0.168
	8	50,624	50,354	50,380	50,453	225	10,091	45	9,864	52	0.089
	10	28,573	28,040	28,313	28,309	168	5,662	34	5,435	41	0.049
	12	15,495	15,467	15,666	15,543	125	3,109	25	2,882	32	0.026

Table 14 (Continued).

Batch no.	Thick- ness in.	Count No. 1	Count No. 2	Count No. 3	Ave. count	Ave. rate	Corr. rate	Normalized rate			
10	Back-ground	1,184	1,182	1,191	1,186	35	237	7			
	0	587,316	589,957	593,085	590,119	770	118,024	154	117,787	161	1.000
	2	333,476	333,918	333,361	333,585	580	66,717	116	66,480	123	0.564
	4	180,188	180,661	180,646	180,498	425	36,099	85	35,862	92	0.305
	6	99,183	98,929	100,133	99,415	316	19,883	63	19,646	70	0.167
	8	55,142	55,218	55,004	55,121	236	11,024	47	10,787	54	0.092
	10	30,199	30,301	30,378	30,293	175	6,059	35	5,822	42	0.050
	12	17,161	17,025	17,148	17,111	131	3,422	26	3,185	33	0.027
11	Back-ground	1,011	1,032	999	1,014	32	203	6			
	0	440,386	440,758	444,970	440,572	666	88,114	133	87,911	139	1.000
	2	246,585	246,327	245,817	246,243	497	49,249	99	48,046	105	0.559
	4	133,988	133,796	134,918	134,234	368	26,847	74	26,644	80	0.303
	6	73,040	72,301	72,590	72,644	270	14,529	54	14,326	60	0.163
	8	40,534	40,769	40,272	40,492	202	8,098	40	7,895	46	0.090
	10	22,821	23,037	22,864	22,843	151	4,569	30	4,366	36	0.050
	12	13,326	13,258	13,218	13,267	115	2,653	23	2,450	29	0.028
12	Back-ground	969	981	960	970	31	194	6			
	0	448,722	449,390	450,032	449,381	671	89,876	134	89,682	140	1.000
	2	255,886	255,557	255,062	255,502	506	51,100	101	50,906	107	0.568
	4	144,563	144,038	143,147	143,933	380	28,787	76	28,593	82	0.318
	6	79,490	79,713	80,192	79,798	283	15,960	57	15,766	63	0.176
	8	45,442	45,544	45,386	45,458	214	9,092	43	8,898	49	0.099
	10	26,238	26,433	26,445	26,372	163	5,274	33	5,080	39	0.057
	12	15,445	15,327	15,365	15,379	124	3,076	25	2,882	31	0.032